Measuring surface currents in lakes with high spatial resolution thermal infrared imagery

Todd E. Steissberg,[1] Simon J. Hook,[2] and S. Geoffrey Schladow[1,3]

Received 7 March 2005; revised 14 April 2005; accepted 5 May 2005; published 8 June 2005.

[1] High spatial resolution thermal infrared satellite images acquired 38 minutes apart from Landsat ETM+ and ASTER were used to measure the surface currents and circulation in Lake Tahoe, California-Nevada, USA. Mean currents of 5–10 cm/s were measured, with maximum currents approaching 35 cm/s. The eastward transport of an upwelling surface jet was clearly apparent, with 15–30 cm/s currents. Three gyres were evident in the vector fields. The satellite image-derived surface currents and circulation patterns are consistent with surface drifter measurements acquired during a different period. These results modify the findings of an earlier study using 1.1 km AVHRR imagery, which concluded there were two counter-rotating gyres in the opposite sense to the two dominant large gyres measured in this study. The high spatial resolution and small time separation allow the surface currents and general circulation in lakes and coastal environments to be accurately quantified using the maximum cross-correlation method. **Citation:** Steissberg, T. E., S. J. Hook, and S. G. Schladow (2005), Measuring surface currents in lakes with high spatial resolution thermal infrared imagery, *Geophys. Res. Lett.*, *32*, L11402, doi:10.1029/2005GL022912.

1. Introduction

[2] Lake and coastal ocean surface feature-tracking typically utilizes moderate-resolution (~1 km) thermal infrared satellite images from a single instrument [*Strub and Powell*, 1986, 1987; *Strub et al.*, 1984]. These data have limited value for current mapping in smaller lakes or certain coastal regions where the spatial resolution of the imagery is insufficient to adequately map the thermal features or track their movement. The recent deployment of high spatial resolution thermal infrared instruments, such as the Advanced Spaceborne Thermal Emission and Reflection Radiometer (ASTER) and Landsat Enhanced Thematic Mapper Plus (ETM+) provides an opportunity to make more detailed measurements of surface temperature, surface currents, and surface circulation in lakes and coastal environments at scales significant to limnological and coastal processes. This study demonstrates the use of a pair of high spatial resolution thermal infrared images acquired from two different sensors (ETM+ and ASTER) 38 minutes apart, to measure the surface currents and circulation in Lake Tahoe, California—Nevada, USA.

1.1. Site Location and Characteristics

[3] Lake Tahoe is approximately 1895 m above mean sea level, in the Sierra Nevada Mountains. The lake is roughly oval in shape. The N-S and E-W axes are 33 km and 18 km long, respectively; the lake has a surface area of 500 km^2. The land portion of the watershed has an area of 800 km^2. Lake Tahoe is considered a deep lake, with an average depth of 330 m and a maximum depth of 501 m. Due to its large volume and proportionately small watershed, Lake Tahoe is a highly oligotrophic (clear, low productivity) lake. It is an ideal natural laboratory; its size and depth make it a good analog for coastal as well as lake systems, and its many cloud-free days and high altitude make it ideal for acquiring remotely sensed data [*Hook et al.*, 2003]. A large body of research exists for Lake Tahoe, primarily due to concern over its diminishing clarity [*Jassby et al.*, 1999], a consequence of increased phytoplankton production and particulate concentrations.

1.2. Satellite Instrument Characteristics

[4] ETM+ has a single thermal infrared band (10.31–12.36 μm) with a spatial resolution of 60 m and NEΔT (noise equivalent temperature difference) of 0.22 K at 280 K [*Barsi et al.*, 2003]. ASTER has five spectral bands in the thermal infrared between 8.125 and 11.65 μm, each with a spatial resolution of 90 m and NEΔT of $\leq$0.3 K at 280 K [*Yamaguchi et al.*, 1998]. ETM+ and ASTER thermal infrared data can be acquired by each sensor twice every 16 days (a day and a night acquisition) at a given location, although ETM+ does not normally record data at night.

1.3. In Situ Measurements

[5] In 1999, a suite of measuring devices was installed at Lake Tahoe to validate the thermal infrared data and products from the ASTER and MODIS (MODerate resolution Imaging Spectroradiometer) instruments on the Terra spacecraft [*Salomonson et al.*, 1989; *Yamaguchi et al.*, 1998]. Meteorological and water temperature measurements are made from four permanently moored buoys on the lake and several stations on the shore [*Hook et al.*, 2003]. Surface drifters, drogued to 2.5 m depth, were deployed for a two-week period, September 20–October 4, 2001, recording their positions every 15 min with integrated Global Positioning System (GPS) boards.

2. Methodology

[6] A pair of ASTER and ETM+ images was acquired June 3, 2001, 38 minutes apart. ETM+ band 6 and ASTER band 13 were corrected to brightness temperature

[1]Department of Civil and Environmental Engineering, University of California, Davis, California, USA.
[2]Jet Propulsion Laboratory, California Institute of Technology, Pasadena, California, USA.
[3]Also at Tahoe Environmental Research Center, University of California, Davis, California, USA.

0094-8276/05/2005GL022912$05.00

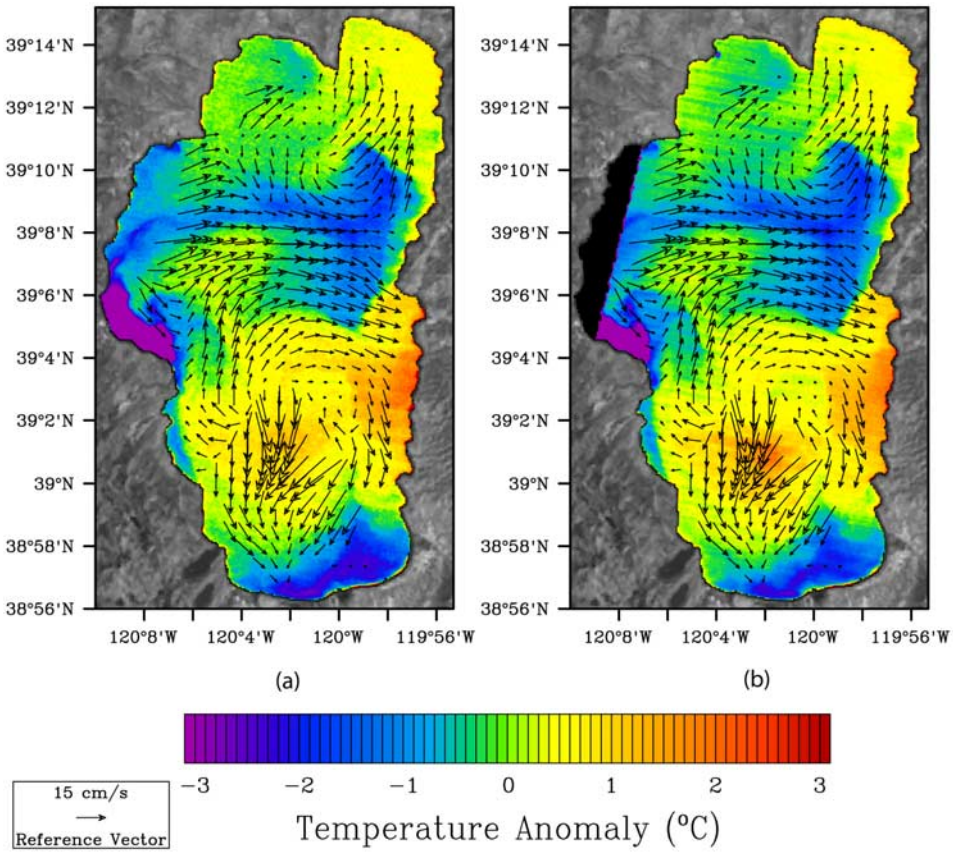

Figure 1. (a) ETM+ Band 6 (high gain) temperature anomaly, June 3, 2001 18:28 UTC. (b) ASTER Band 13 temperature anomaly, June 3, 2001 19:06 UTC. The ETM+ image was interpolated to a 90 m grid using bilinear interpolation. The satellite image-derived surface current vector field is overlaid on both images.

(emissivity = 1.0), registered to a base map, projected to a Universal Transverse Mercator (UTM, Zone 10) projection, and then linearly interpolated to a 90 m grid. ASTER band 13 was chosen due to its lower noise and reduced striping.

[7] The maximum cross-correlation method [*Bowen et al.*, 2002; *Emery et al.*, 1986; *Ninnis et al.*, 1986] was employed for surface feature tracking. The brightness temperature images were low-pass filtered with a 9 × 9 filter, to remove image striping and sensor noise, and then detrended by computing the centered-difference gradients [*Emery et al.*, 1986] to improve feature tracking. Other studies [*Emery et al.*, 1992; *Tokmakian et al.*, 1990] obtained superior results for ocean currents using raw brightness temperatures. Computing the gradients provided superior tracking for the images presented here, as determined by visual change detection and comparison with circulation patterns indicated by surface drifter measurements. This could be due to the smaller temperature range and relatively weaker thermal gradients in the lake images than in ocean images [*Emery et al.*, 1992]. Thermal features were tracked by comparing the correlation coefficients between moving template windows in both images. A 41 × 41 pixel template was selected for feature tracking, ensuring enough points for accurate correlation computations while facilitating the tracking of mesoscale features.

[8] To determine the minimum acceptable correlation coefficient, the average autocorrelation function was computed and plotted (not shown) for both images. While asymmetric, these indicated an approximate autocorrelation length scale of 30 pixels (2.7 km). Dividing the number of points in the template (1681) by the autocorrelation length scale yielded 54 degrees of freedom. At the 99% confidence level, correlation coefficients greater than 0.35 are significant. Velocity vectors were not computed for correlation coefficients below this threshold. Where present, land and other non-water pixels were removed from the templates. To allow for current determination near the shoreline [*Emery et al.*, 1992], templates containing up to 40% non-water pixels were used in the computations. Minimum acceptable correlation coefficients were increased in accordance with the number of non-water pixels present in templates.

[9] The search region was sized according to the maximum expected displacement. Surface drifter measurements in Lake Tahoe, acquired September 2001, indicate typical currents of 5–15 cm/s during the stratified period, with maximum currents near 30 cm/s. After discarding an outlier of 40 cm/s, the surface drifters indicated a maximum velocity of 28.3 cm/s. Since currents at the skin can be approximately 25% larger than at 2.5 m depth [*Koçyigit and Falconer*, 2004], a maximum velocity of approximately 35 cm/s is possible at the skin. Therefore, a 59 × 59 pixel search region was selected, yielding a maximum orthogonal displacement of 9 pixels (8.1 km) and maximum orthogonal velocity components of 35.5 cm/s. However, spurious

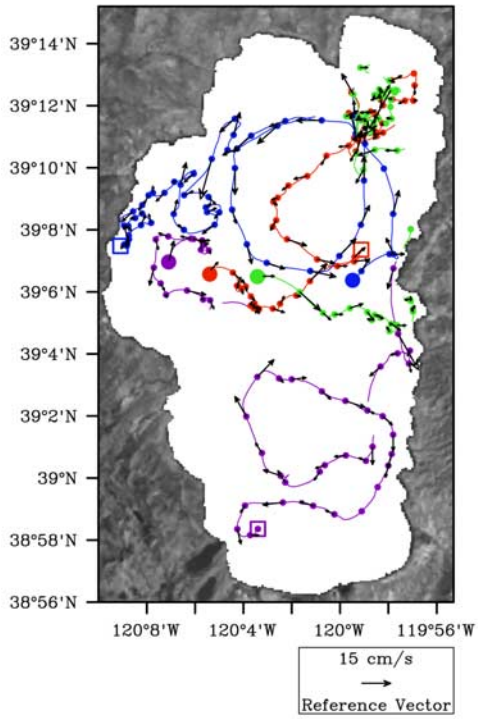

Figure 2. GPS-tracked surface drifters, drogued to 2.5 m depth, September 20, 2001–October 4, 2001. Colored dots indicate each drifter's position at 6 hr intervals. Large colored circles denote drifter deployment while squares denote drifter retrieval.

velocities up to 50 cm/s are possible along non-orthogonal directions. Therefore, search templates yielding velocities above 36 cm/s were rejected, allowing computation with other templates at lower but statistically significant correlations. A geolocation error of ±1 pixel gives a maximum expected error of 3.9 cm/s.

[10] Vectors were computed for templates centered on every tenth pixel in the first image, comparing each template in the first image with templates centered on each pixel, in turn, in the 59 × 59 pixel search region in the second image. The template in the second image that produced the maximum cross-correlation coefficient was used to compute the velocity vector, multiplying the displacement in pixels by the pixel size (90 m) and dividing by the elapsed time (38 min). Spurious data vectors were identified by a deviation in a vector component by more than 3 standard deviation units from the median of a 3 × 3 array surrounding the vector. The erroneous vector components were replaced by the median of the 3 × 3 array. The resulting vector field was low-pass filtered with a 3 × 3 filter.

3. Discussion

[11] For each daytime ASTER image, there typically exists a corresponding daytime ETM+ image acquired approximately 40 minutes earlier. Figures 1a and 1b show an ETM+/ASTER image pair acquired 38 minutes apart on June 3, 2001, displayed as temperature anomaly, obtained by subtracting the median brightness temperature from each image, to compensate for differences in temperature due to diurnal heating or cooling. Missing pixels (Figure 1b) were masked in black. Dates and times given for all data are in UTC. Standard local time (Pacific Standard Time) is UTC minus eight hours.

[12] The images show a large partial upwelling event, resulting from sustained 9–11 m/s winds from the southwest. The patterns in these images indicate that cool, metalimnetic water has upwelled on the west (upwind) side of the lake as a distinct jet. The water masked in dark purple along the western shore of the June 3, 2001 images is more than 4°C cooler than the median temperature of the water surface.

[13] The surface current vector field computed from these images was overlaid on the ETM+ and ASTER images in Figure 1. Mean currents of 5–10 cm/s are evident, with maximum currents approaching 35 cm/s. The east-to-west transport of the surface jet is clearly shown, with currents of 15–30 cm/s. Also, a counter-clockwise circulation pattern is evident in the northern section of the lake, with a clockwise circulation pattern in the southern section of the lake. Of the total number of water pixels, 98% had correlation coefficients greater than 0.35, 94% greater than 0.5, and 68% greater than 0.8. The predicted currents near 39°01′N, 120°02′W were larger than expected. However, these correspond to the displacement of the strong warm feature visible in the images, and were predicted with correlation coefficients of 0.43 to 0.52.

[14] Surface drifter measurements (Figure 2) (not coincident with images), show similar circulation patterns, with dominant counter-clockwise circulation in the northern section of the lake and clockwise circulation in the central to southern section of the lake. The surface drifter data also indicate the possible presence of a third smaller gyre in the southern section of the lake, as also indicated by a divergence in the vector field near the southwest shore (Figure 1). Average surface currents measured by surface drifters were approximately 5–10 cm/s, with maximum currents above 28 cm/s. The surface drifter velocities were generally lower than the image-derived velocities, which can be accounted for by the reduction of velocity with depth [*Koçyigit and Falconer*, 2004] and wind speeds less than 8 m/s throughout most of the deployment period, while the winds immediately preceding the satellite image acquisitions were 9–11 m/s. The elevated surface drifter velocities approaching 28 cm/s followed sustained winds of 9–12 m/s. While the satellite-derived vector field provides a snapshot of the surface currents following elevated winds, the surface drifters indicate a sustained circulation over a two-week period with patterns similar to those measured using the satellite images.

[15] MODIS images (not shown) acquired ~11 hr apart on June 3 (concurrent with the ASTER image) and June 4, 2001, provide further evidence of the large-scale gyral transport as the cool jet diverges northward and southward along the eastern shore. However, the relatively large pixel size of MODIS (1 km) limits applicability of the maximum cross-correlation method on all but the largest lakes. Furthermore, the large time separation between the MODIS images allowed significant thermal pattern change through rotation, diffusion, sinking, and diurnal heating and cooling.

[16] High-resolution ASTER and ETM+ images facilitate fine-scale surface current determination not achievable

using moderate-resolution instruments. Previous researchers [*Strub and Powell*, 1986, 1987], using 1.1 km AVHRR (Advanced Very High Resolution Radiometer) imagery and a different technique suggested the existence of two large counter-rotating gyres, in the opposite sense to the dominant northern and south-central gyres measured in this study, at a time of similar wind conditions. Furthermore, the results presented here demonstrate eastward transport of upwelled water near mid-lake, while the earlier study concluded that upwelled water was transported eastward along the northern shore, with westward flow near mid-lake. It is possible that the effects of moderate-resolution imagery with large time-separations between them and the presence of multiple gyres could result in anomalous interpretation.

4. Summary and Conclusions

[17] A methodology utilizing high spatial resolution thermal infrared images from ASTER and ETM+ to measure surface currents and circulation patterns at scales relevant to lakes and coastal systems is presented. Since surface currents distribute nutrients, phytoplankton, and contaminants in lakes and coastal environments, employing high-resolution thermal infrared imagery to track surface currents can lead to better understanding of ecological functioning and environmental degradation in these systems. Using cross-platform measurements reduces the elapsed time between images, eliminating diurnal heating and cooling effects, as well as reducing the nonlinear effects of rotation and deformation, and three-dimensional effects of large-scale upwelling and downwelling. When combined with the high resolution of the thermal infrared channels of ASTER and ETM+, the surface currents and general surface circulation in lakes and coastal environments can be properly quantified.

[18] **Acknowledgments.** This research was carried out in part at the Jet Propulsion Laboratory, California Institute of Technology, under a contract with NASA. The work by T. Steissberg was funded by a NASA Earth System Science Fellowship and by the NSF under grant OCE-9907557.

References

Barsi, J. A., J. R. Schott, F. D. Palluconi, D. L. Heider, S. J. Hook, B. L. Markham, G. Chander, and E. M. O'Donnell (2003), Landsat TM and ETM+ thermal band calibration, *Can. J. Remote Sens.*, *29*(2), 141–153.

Bowen, M. M., W. J. Emery, J. L. Wilkin, P. C. Tildesley, I. J. Barton, and R. Knewtson (2002), Extracting multiyear surface currents from sequential thermal imagery using the maximum cross-correlation technique, *J. Atmos. Oceanic Technol.*, *19*(10), 1665–1676.

Emery, W. J., A. C. Thomas, M. J. Collins, W. R. Crawford, and D. L. Mackas (1986), An objective method for computing advective surface velocities from sequential infrared satellite images, *J. Geophys. Res.*, *91*, 12,865–12,878.

Emery, W. J., C. Fowler, and C. A. Clayson (1992), Satellite-image derived Gulf-Stream currents compared with numerical-model results, *J. Atmos. Oceanic Technol.*, *9*(3), 286–304.

Hook, S. J., F. J. Prata, R. E. Alley, A. Abtahi, R. C. Richards, S. G. Schladow, and S. Ó. Pálmarsson (2003), Retrieval of lake bulk and skin temperatures using Along-Track Scanning Radiometer (ATSR-2) data: A case study using Lake Tahoe, California, *J. Atmos. Oceanic Technol.*, *20*(4), 534–548.

Jassby, A. D., C. R. Goldman, J. E. Reuter, and R. C. Richards (1999), Origins and scale dependence of temporal variability in the transparency of Lake Tahoe, California-Nevada, *Limnol. Oceanogr.*, *44*, 282–294.

Koçyigit, M. B., and R. A. Falconer (2004), Three-dimensional numerical modelling of wind-driven circulation in a homogeneous lake, *Adv. Water Resour.*, *27*(12), 1167–1178.

Ninnis, R. M., W. J. Emery, and M. J. Collins (1986), Automated extraction of pack ice motion from Advanced Very High-Resolution Radiometer imagery, *J. Geophys. Res.*, *91*, 725–734.

Salomonson, V. V., W. L. Barnes, P. W. Maymon, H. E. Montgomery, and H. Ostrow (1989), MODIS: Advanced facility instrument for studies of the Earth as a system, *IEEE Trans. Geosci. Remote Sens.*, *27*(2), 145–153.

Strub, P. T., and T. M. Powell (1986), Wind-driven transport in stratified closed basins: Direct versus residual circulations, *J. Geophys. Res.*, *91*, 8497–8508.

Strub, P. T., and T. M. Powell (1987), Surface temperature and transport in Lake Tahoe: Inferences from satellite (AVHRR) imagery, *Cont. Shelf Res.*, *7*, 1001–1013.

Strub, P. T., T. M. Powell, and M. R. Abbott (1984), Temperature and transport patterns in Lake Tahoe: Satellite imagery, field data and a dynamical model, *Verh. Int. Ver. Limnol.*, *22*, 112–118.

Tokmakian, R., P. T. Strub, and J. McClean-Padman (1990), Evaluation of the maximum cross-correlation method of estimating sea surface velocities from sequential satellite images, *J. Atmos. Oceanic Technol.*, *7, 852–865.*

Yamaguchi, Y., A. B. Kahle, H. Tsu, T. Kawakami, and M. Pniel (1998), Overview of Advanced Spaceborne Thermal Emission and Reflection Radiometer (ASTER), *IEEE Trans. Geosci. Remote Sens.*, *36*(4), 1062–1071.

S. J. Hook, Jet Propulsion Laboratory, California Institute of Technology, Pasadena, CA 91109, USA.

S. G. Schladow and T. E. Steissberg, Department of Civil and Environmental Engineering, University of California, Davis, CA 95616, USA. (tsteissberg@ucdavis.edu)